Advanced Composites and Hybrid Materials (2021) 4:212–222
https://doi.org/10.1007/s42114-020-00188-8

ORIGINAL RESEARCH

Investigation of microstructure and selected properties of Al_2O_3-Cu and Al_2O_3-Cu-Mo composites

Justyna Zygmuntowicz[1] · Joanna Łoś[2] · Bernard Kurowski[2] · Paulina Piotrkiewicz[1] · Waldemar Kaszuwara[1]

Received: 22 June 2020 / Revised: 13 October 2020 / Accepted: 10 November 2020 / Published online: 20 November 2020

Abstract

The scope of work included the fabrication of ceramic-metal composites from the Al_2O_3-Cu and Al_2O_3-Cu-Mo and examining their microstructure and selected properties. The composites were fabricated by the slip casting method. The rheological behavior, microstructures, X-ray analysis, and mechanical properties were investigated. The rheological study demonstrated that all of the obtained slurries were non-Newtonian shear diluted fluids and stability on time. In both slurries, the flow limit is close to 0 Pa, which is very beneficial when casting the suspensions into molds. The X-ray analysis reveals Al_2O_3, Cu, and Mo phases in all specimens. No new phases were found in both types of composites after the sintering process. The results provided that the hardness for Al_2O_3-Cu-Mo composites was equal to 10.06 ± 0.49 GPa, while for Al_2O_3-Cu, it was equal to 6.81 ± 2.08 GPa. The K_{1C} values measured, with the use of Niihara equation, for composites with and without the addition of Mo were equal to 6.13 ± 0.62 MPa $m^{0.5}$ and 6.04 ± 0.55 MPa $m^{0.5}$, respectively. It has been established that the mean specific wear rates of Al_2O_3-Cu and Al_2O_3-Cu-Mo samples were 0.35 × 10–5 ± 0.02 mm^3 N^{-1} m^{-1} and 0.22 × 10–5 ± 0.04 mm^3 N^{-1} m^{-1}, respectively. It was found that molybdenum addition improved wear resistance properties of the composites.

Keywords Composites · Slip casting · Mechanical properties · Scanning electron microscopy

1 Introduction

One of the most challenging objectives in modern engineering is the continuous design and development of advanced materials for high-performance applications. Advanced ceramics due to the wide range of current and future applications can be considered one of the main directions in the advancement of this challenge. Despite remarkable mechanical properties, such as high hardness and wear resistance, high Young's modulus, chemical stability, and thermal shock resistance of the advanced ceramic materials, their use in engineering is limited. Low toughness and plasticity, in comparison to the metals, in combination with high sensitivity for the presence of flaws in the structure effectively exclude ceramics from high-performance applications. Considering the above, the necessity for new ceramic-based materials with enhanced properties has been clearly demonstrated [1–3].

Composites and especially ceramic-metal composites may be considered a possible solution. In the last decade, a lot of attention has been paid to composites [4–7]. This group of composites successfully combines the advantageous properties of individual components—ceramic and metal—allowing to obtain new material with completely different, promising properties with a wide range of possible applications. For this reason, fabrication of ceramic-metal composites still constitutes a research field addressing a lot of interest [1–3].

Alumina is one of the widely used engineering ceramic materials. Its low density, high hardness, and thermal and chemical stability combined with the ductility of the metal particles result in the composite material with promising properties [8, 9]. Moreover, the literature data shows that the application of ceramic nanostructures in composites is an important factor for environmental remediation [10–13]. Nowadays, it is important to pay attention to the selection of components on the ecological aspects. Multiple research proved that the incorporation of the ceramic matrix with even a small amount of ductile metal particles significantly enhances the toughness of the final composite. The dispersion of metal particles such

✉ Justyna Zygmuntowicz
Justyna.zygmuntowicz@pw.edu.pl

[1] Faculty of Materials Science and Engineering, Warsaw University of Technology, 141 Woloska Str., 02-507 Warsaw, Poland

[2] Institute of High Pressure Physics of the Polish Academy of Sciences, 29/37 Sokolowska Str., 01-142 Warsaw, Poland

as Ni [14–16], Mo [17, 18], Ag [19], W [20], and Cu [21–28] in the ceramic alumina matrix was investigated and in all has been found to improve the fracture toughness of obtained composites.

Due to the high ductility combined with proper thermal and electrical conductivity of Cu particles, alumina/copper system has a permanent scientific interest. It is believed that favorable properties of both components enable to fabricate composite with enhanced both mechanical properties and conductivity. Improvement of the ceramic/metal properties, based on the reinforcement models, indicated the need for a homogenous distribution of small metal inclusions in the ceramic matrix in order to fabricate composite material with desired properties [21].

The review of specialist literature on this system indicated that Al_2O_3-Cu ceramic-metal composites can be successfully obtained with the use of different manufacturing methods such as hot pressing [22–25], uniaxial pressing with pressureless sintering [27], or slip casing [28]. Research study made by Oh et al. on the alumina/copper system allowed characterizing composite samples fabricated with the use of hot-pressing procedure [22–25]. Three different fabrication processes were applied to obtain powder mixtures. First, one commercially available Cu powder was used as a source of Cu particles in metal phase. The other two were based on obtaining copper particles as a result of CuO powder reduction [22, 26] or calcination and reduction of Cu nitrate [26]. It was noted that powder mixture preparation influences the microstructure and properties of hot-pressed Al_2O_3-Cu composites and thus mechanical property enhancement can be obtained by using Al_2O_3-CuO and Al_2O_3-Cu nitrate more effectively. J.G. Miranda-Hernandez et al. analyzed the correlation between microstructure and mechanical properties in alumina/copper composites with different copper contents in the metal phase. Composites were manufactured by the combination of mechanical alloying and pressureless sintering with the use of commercially available alumina and copper powders. The research revealed that liquid copper during the sintering process goes inside the bulk of the sample results in densification enhancement and porosity elimination. An increase in copper content also caused the decrease of hardness with fracture toughness and conductivity improvement at the same time [27]. In the research made by M. Stratigaki et al., alumina/copper composites with different metal particle contents were fabricated with the use of slip casting technique. Commercially available powders and deflocculant enable authors to obtain alumina/copper samples with good relative density and homogenous spatial distribution of metal particles. It was observed that increasing the Cu amount in the composite results in impact resistance behavior enhancement with limited loss of stiffness and hardness. Scientific knowledge to date allows for following statements that the optimum combination of properties was observed for composites with low Cu particle amount (under 5 vol%.) [28].

Available specialist literature has proven that the addition of the small amount of copper to the ceramic Al_2O_3 matrix results with mechanical property enhancement [22, 27, 28] and higher thermal shock resistance in comparison to the monolith Al_2O_3 [24, 27]. Metal particles were also observed to cause significantly inhibited grain growth of the Al_2O_3 matrix [22]. Significant for this particular composite system is the fact that the copper melting point (1084 °C [29]) during the consolidation process is below the usual sintering temperature of the matrix. Due to the poor wettability between copper and alumina, molten copper shows a tendency to remain spherical in shape. A combination of the above with the difference in thermal expansion coefficients of the components may interfere with the proper adhesion at the Al_2O_3-Cu interface. This can also cause part of the reinforcement to flow out from the material during the sintering [30–32].

The research in this manuscript focused on fabrication ceramic-metal composites from the ternary Al_2O_3-Cu-Mo system and examination of the second metal phase addition influence on selected physical and mechanical properties of the samples. The slip casting method was used to prepare Al_2O_3-Cu-Mo composites with 15 vol% of metal content. This technique is widely used in ceramic manufacturing due to its effectivity, good initial particle package in green bodies in comparison to the conventional dry-pressing methods [33], and the possibility to obtain complex-shaped and large-sized materials [34–36]. The present study attempts to evaluate the influence of Mo particle addition as a second component of the metal phase in the composite on the microstructures and selected properties were investigated. The rheological behavior of prepared suspensions used to fabricate composites was studied. Selected physical and mechanical properties like hardness, fracture toughness, and tribological behavior of the obtained composite and the correlation between the microstructure and mechanical properties were examined. First of all, we believe that the investigation presented in this manuscript will give a starting point for other scientists to produce composites from the Al_2O_3-Cu-Mo system. In addition, we hope that this research regarding the additive of Mo to Al_2O_3-Cu composites will lead to improvements in the physical and mechanical properties of ternary composites from the ceramic-metal system for a broad range of applications. In summary, the results obtained will allow determining the relation between microstructure, phase structure, and basic properties of the Al_2O_3-Cu in comparison to Al_2O_3-Cu-Mo.

2 Experimental procedure

The research has been carried out on alumina, copper, and molybdenum powders. The Al_2O_3 TM-DAR (Tamei Chemicals, Japan) powder was high purity of an average

particle size 126 ± 13 nm (measured on Zetasizer Nano ZS, Malvern Instruments), density 3.80 g cm^{-3} measured on AccuPyc II 1340 Pycnometer (Micromeritics, USA), and a specific surface area 10.85 ± 0.07 m^2 g^{-1} (calculated from BET). The SEM image (Fig. 1a) reveals that the Al_2O_3 particles are characterized by spherical morphology. It was found that alumina powders were firmly agglomerated. The mean particle size distribution determined by dynamic laser scattering (DLS) for copper (Sigma-Aldrich, Poland) was estimated to be 15.4 ± 5 μm, whereas molybdenum (Createc, Poland) powder was 13.4 ± 5 μm. The metal powders characterize by high purity equal 99.99%. Analysis of the images of the morphology reveals that cooper powder has close to a spherical shape (Fig. 1b). As can be seen in the SEM images, Mo powder has an irregular shape (Fig. 1c). The specific surface area for the copper powder was 0.29 ± 0.01 m^2 g^{-1}, whereas the molybdenum powder characterizes by a specific surface area equal to 0.24 ± 0.01 m^2 g^{-1} (calculated from BET). As organic additives, there were used di-ammonium hydrogen citrate (DAC) and citrate aside (CA) delivered by POCH SA. Distillate water was used as a solvent in the experiment to produce the composites.

The two series: Al_2O_3-Cu (series I) and Al_2O_3-Cu-Mo (series II) composites were prepared with the use of slip casting method. The composite specimens were obtained according to the slip casting technique schematically shown in Fig. 2. In this study, suspensions with 50 vol% of solid content were fabricated. A total metal share in the composite system was 15 vol%. In the case of three-component system, the ratio of Cu to Mo was 1:1.

The mixture of the slip casting components was fabricated in several steps. In the first step, the dispersing agents were dissolved in distilled water. The addition of 1.5 wt% of the dispersing agents (DAC and CA) allows obtaining the slurries which are flowable and stable over time. Then, ceramic and metallic powders were added. The prepared slurries were mixed and degassed in a planetary centrifugal mixer THINKY ARE-250. The suspensions were heterogeneous for 8 min at the rate of 1000 rpm and then degassed for 2 min at the rate of 2000 rpm. In the next stage, the mixture was then cast into identical gypsum molds. The use of porous molds permitted the removal of water from the prepared slurries as a result of the capillary action force which resulted in the green body. In the next stage, the mixture was then cast into identical gypsum molds and the obtained specimens were

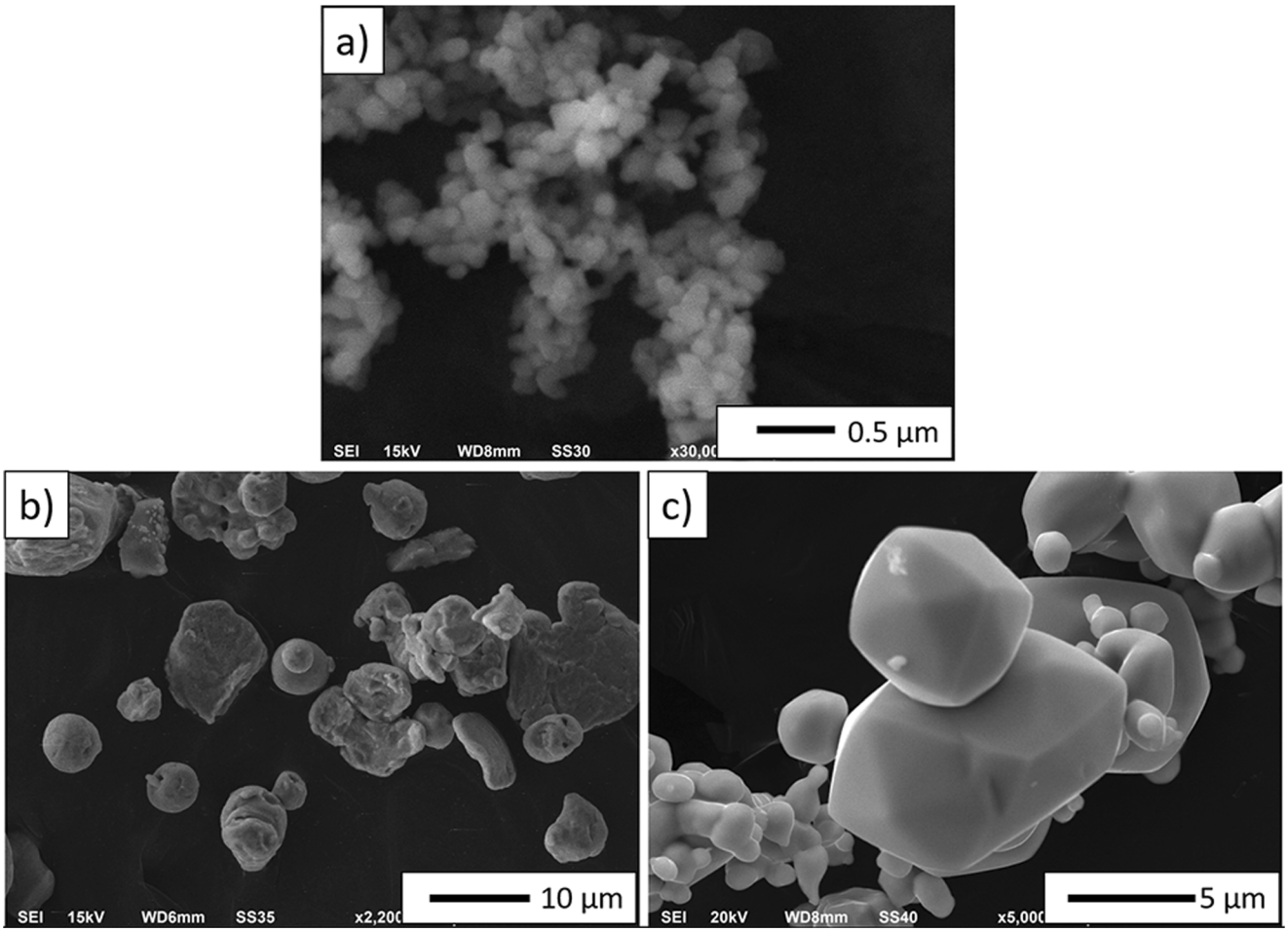

Fig. 1 The morphology of the base powders. **a** Al_2O_3. **b** Cu. **c** Mo

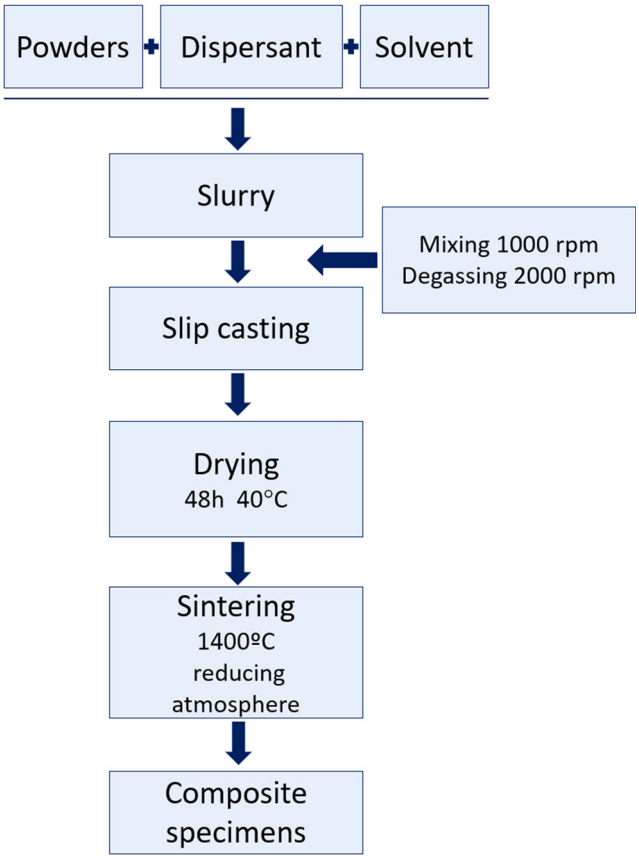

Fig. 2 The processing routs used for the preparation of samples by slip casting method

dried for 48 h at 40 °C in the laboratory dryer. The dried and shrunk sample could be removed from the gypsum mold easily. The sample was sintered at 1400 °C in reducing atmosphere (80% N_2 and balance H_2). The dwell time of the composites is 2 h. During the sintering, the heating and cooling rate was 2 °C min^{-1}. The selection of the sintering temperature in the experiment was determined by the low melting point of copper equal to 1084 °C [29] as one of the metal phase components. The use of a lower sintering temperature will prevent liquid metal from leaking during the sintering process.

Several methods were used to establish the properties of the slurries and microstructure and selected properties of the obtained composites.

The stability of the suspension during the fabricated samples by the slip casting method is significant. Therefore, macroscopic observation of two slurries Al_2O_3-Cu (series I) and Al_2O_3-Cu-Ni (series II) during the sedimentation test was made. Slurry samples with volumes of 15 mL were poured into individual test tubes. The experimental time was 48 h. The sedimentation test was conducted at room temperature (25 °C), and images were gained with a digital camera every 2 h.

The rheological measurements are an enormously serviceable technique for investigating shear stress as a function of shear rate and viscosity as a function of the applied shear rate [33, 37]. Rheological tests enable the characterization of tested fluids [38, 39]. Such measurements make it possible to determine what kind of fluid it is [40–42]. Furthermore, the results of rheological tests allow statements, which fabricated slurry characterizing the highest or lowest viscosity. For this purpose, the viscosity of slurry was studied by the Kinexus Pro rheometer (Malvern Instruments, UK) equipped with plate-plate geometry. The diameter of the rotating geometry was 40 mm with the gap between plates equal to 0.5 mm. During the investigation, the value of the shear rate was increased from 0.1 to 300 s^{-1}. The measurements were done at 25 °C.

An examination of the essential characterization of the produced composites was conducted.

A scanning electron microscope (JSM-6610 SEM) was employed to characterize the microstructure of the composites. The samples were ground and polished to see the metal phases clearly in SEM investigation and to eliminate the effect of surface flaws on mechanical properties. The composites mounted in resin were ground with abrasive paper in the range of 80 to 4000 gradations and polished using diamond pastes: 3 μm and 1 μm gradation. Before observations, samples were carbon coated using Quorum Q150T ESS coating system. The chemical compositions were characterized by using energy-dispersive X-ray spectroscopy detector. EDX chemical composition analyses of the specimens were done at acceleration voltage 15 kV.

The phase analysis was carried out by X-ray diffractometry (XRD) at sweep rates of 0.02° and counting time of 0.5 min^{-1} with a 2θ range from 20 to 100° by a Rigaku MiniFlex II diffractometer. The analysis was performed with Cu Kα: $\lambda = 1.54178$ Å, 30 kV, 15 mA.

The selected physical properties of the sintered specimens were measured by the Archimedes method.

In this study, the hardness and fracture toughness were measured with a Vickers hardness tester (WPM LEIPZIG HPO-250) with the use of the indentation method under the load of 196 N, calculated from the length of cracks which developed during a test using Anstis and Niihara equations [43–46]. In the presented work, the fracture toughness has been calculated based on two formulas [43–46]:

- Anstis equation for $l/a > 1.5$:

$$K_{\mathrm{Ic}} = 0.016\left(\frac{E}{\mathrm{HV}}\right)^{0.5} \cdot \frac{P}{c^{1,5}} \tag{1}$$

- Niihara equation for $0.25 < l/a < 2.5$:

$$K_{\mathrm{Ic}} = 0.018 \cdot \mathrm{HV}^{0.6} \cdot E^{0.4} \cdot 0.5d \cdot l^{-0.5} \tag{2}$$

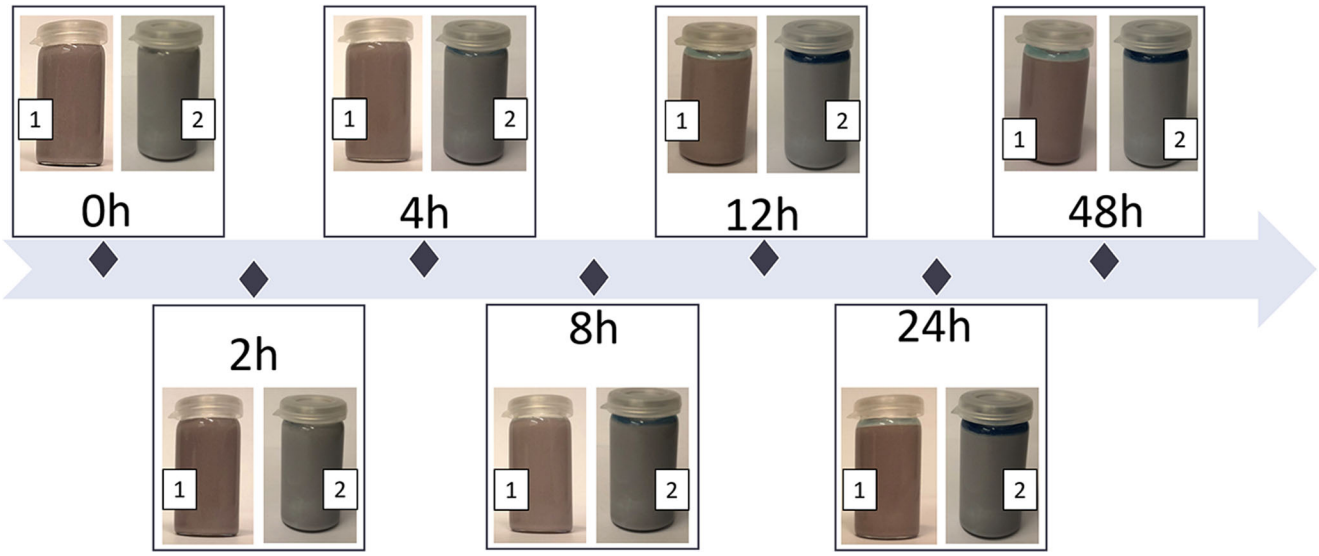

Fig. 3 Sedimentation behavior of the suspension Al_2O_3-Cu (1) and Al_2O_3-Cu-Mo (2) in time

where in the Anstis equation, E is the Young's modulus (GPa), HV is the Vickers hardness (GPa), P is the indentation load (kgf), and c is the crack length from the center of the indentation to the crack tip (mm), while in the Niihara equation, H is the Vickers hardness (GPa), E is the Young's modulus (GPa), d is the diagonal of the Vickers indentations (mm), and l is the average crack length (mm) [43–46].

Friction is one of the most common physical phenomena in nature and one of the main processes occurring between moving elements, which leads to energy losses and wear-related losses. The wear usually causes the need to replace elements, assemblies, or entire machines. Research on friction processes and implementation of its results is of a great importance for improving the economic and energy efficiency of enterprises using machines in the production process. The wear resistance tests allow predicting the behavior and durability of elements in the work environment better. They are the basic tool in mechanical design of machine components.

The ball on disc tribological tests were performed using The Bruker's Universal Mechanical Tester (UMT) TriboLab™. Its 2-dimensional force sensor DFH-20 enables measurements in the load range from 2 to 200 N with 10-mN resolution. Measurements of friction force and normal force allowed obtaining the coefficient of friction (COF) of specimens. The WC ball of 9.5-mm diameter was used as a counterbody. The balls' holder was idle during the whole experiment. After fixing rigidly to rotating holder, unlubricated samples were tested under a constant load of 100 N for 10 h at ambient conditions. Circular wear tracks with a 5-mm diameter were formed on the tested samples. Tests were carried out at a revolution speed of 300 rpm, which corresponds to about 0.16 m s^{-1}. The sliding distance equaled 5760 m. The measured data were recorded every 0.01 s.

All samples were weighed before and after tribological testing. Change in mass Δ of tested samples was determined with Mettler Toledo Analytical Balance with readability down to 0.1 mg.

The wear volume V (mm^3) was calculated as quotient of specimen's weight loss Δm (g) and its density ρ (g cm^{-3}). The specific wear rate w was defined according to the standard ISO 20808:2016 as the volume loss V per distance L (m) and the applied load F_n (N):

$$w = \frac{V}{LF_n} \tag{3}$$

The values of the coefficient of friction, the wear volume, and the specific wear rate were calculated as a mean of results collected for 5 samples.

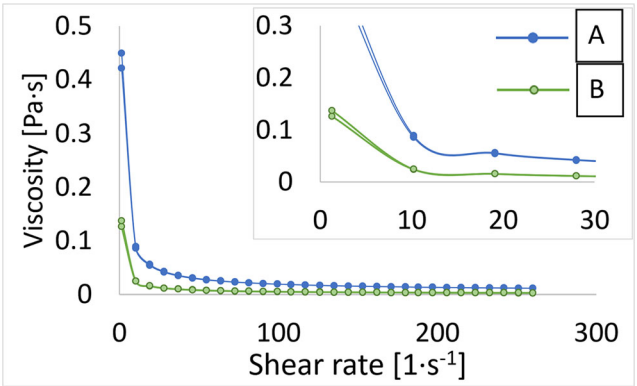

Fig. 4 The viscosity of the prepared suspensions: Al_2O_3-Cu (marked on the chart as A) and Al_2O_3-Cu-Mo (marked on the chart as B) as a function of shear rate

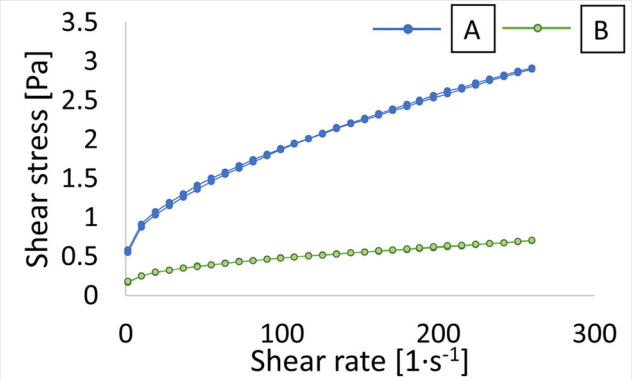

Fig. 5 Flow curves of the composites slurry: Al_2O_3-Cu (marked on the chart as A) and Al_2O_3-Cu-Mo (marked on the chart as B)

3 Results and discussion

Figure 3 shows the collected photos during the sedimentation test. This experiment demonstrates that even after 4 h, both slurries were stable and any phase separation was not noticed. During the investigation time, in the case of Al_2O_3-Cu-Mo suspensions after 8 h, slight sedimentation was observed in contrast to the Al_2O_3-Cu suspension, which was stable throughout the experiment. Conceivably worse the stability over time of a slurry containing molybdenum is due to Mo density, which promotes the particle molybdenum sedimentation in the suspensions. These results demonstrated that particles were dispersed well in Al_2O_3-Cu slurry even after 48 h. Nevertheless, the obtained results show that both suspensions may be suitable for forming composites by the slip casting method since they are stable for a minimum of 2 h from the moment of mass preparation.

The results of the rheological experiments have been collected in Fig. 4 and Fig. 5. On the basis of viscosity results shown in Fig. 4, it was reported that both suspensions are shear of the thinning fluid. It was found that the Al_2O_3-Cu slurry (marked on the chart as A) has a maximal viscosity equal to 0.421 Pa s at a minimal shear rate of 1.3 s^{-1}. It was observed that when the shear rate increases to 260 s^{-1}, the viscosity decreases to about 0.0112 Pa s. However, on the basis of Fig. 4, it was found that Al_2O_3-Cu-Mo suspension (marked on the chart as B) has a maximal viscosity equal to 0.26 Pa s at a minimal shear rate of 1.3 s^{-1}. It was found that when the shear rate increases to 260 s^{-1}, the viscosity decreases to about 0.0027 Pa s. These results lead to the conclusion that the addition of molybdenum particles reduces the

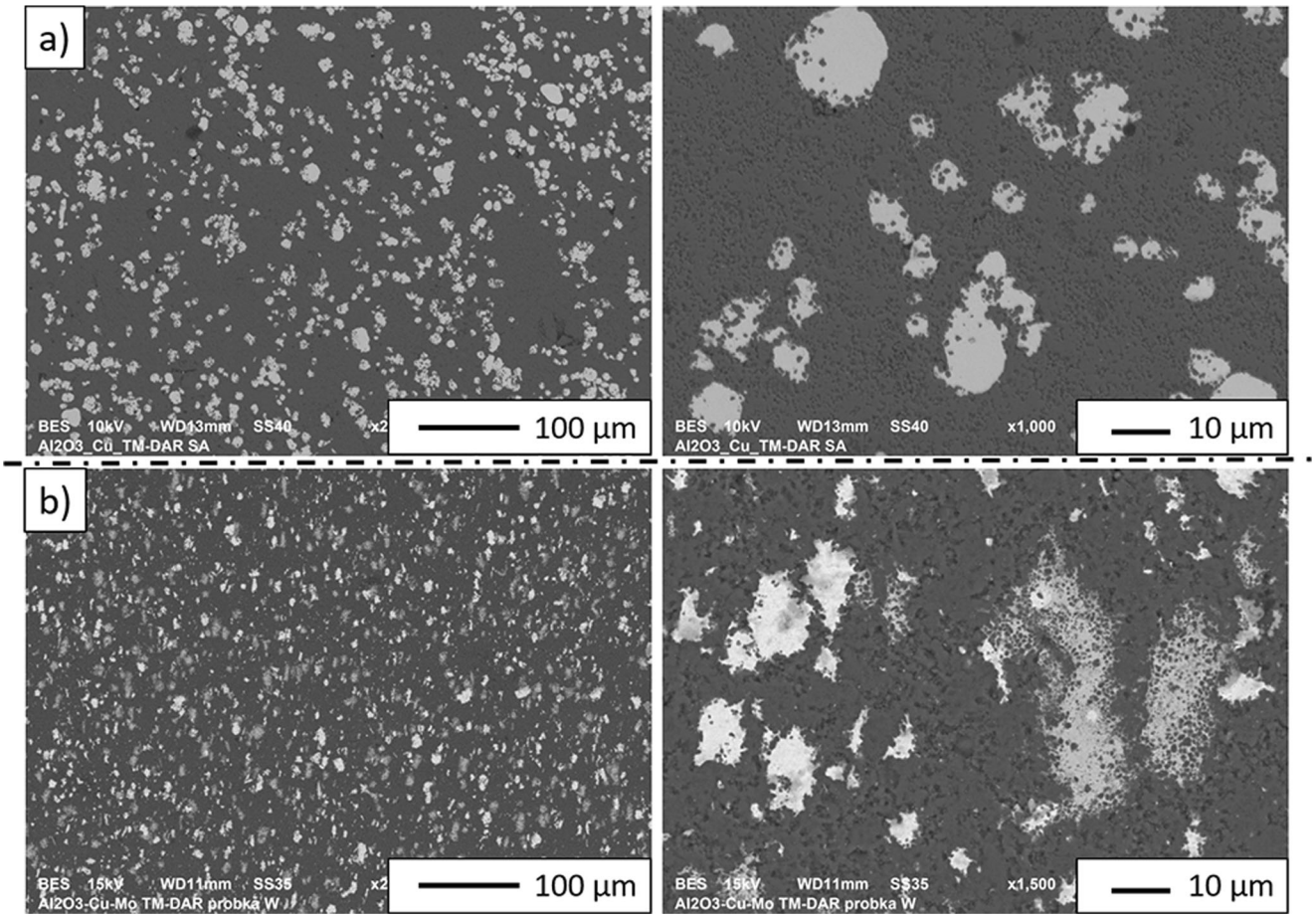

Fig. 6 SEM images of sintered composites. **a** Al_2O_3-Cu. **b** Al_2O_3-Cu-Mo

viscosity of the suspension compared to a slurry containing alumina and copper.

The flow curves of the suspensions shown in Fig. 5 provided evidence of both produced slurries exhibiting antithixotropic behavior (rheopexy). It may be concluded that the molecular structure appears in the suspensions which causes an increase of viscosity. This is due to the existence of metal particles (Cu or Cu and Mo) in the alumina particle suspension and they are electrostatic interactions. The flow curves in Fig. 5 demonstrated that for Al_2O_3-Cu suspensions, the minimum shear rate of 1.3 s^{-1} shear stress was 0.547 Pa, while the maximum shear rate of 260 s^{-1} shear stress was 2.9 Pa. For Al_2O_3-Cu-Mo slurry, the flow curves provided information that the minimum shear rate of 1.3 s^{-1} shear stress was 0.164 Pa, while the maximum shear rate of 260 s^{-1} shear stress was 0.7 Pa. The resulting suspensions were distinguished by high fluidity. The measurements have shown that the flow limit is close to 0 Pa in both suspensions, which is very beneficial when casting the slurries into molds.

The microscopic observations were carried out on cross-sectioned fragments of the samples and the images are shown in Fig. 6. It has been determined that the distribution of the metallic phase in the examined specimens has a homogeneous character. The darker regions on samples revealed on the micrographs correspond to the ceramic matrix, while the bright areas are metal phases. The performed scanning electron microscopy observations revealed changes in the microstructure of the samples depending on the composition of composites. It was found that in the case of Al_2O_3-Cu composites, the metal phase particles have gentle edges and their morphology did not change significantly compared to the initial Cu powder. However, in the case of the ternary composite, it was found that the metallic phase particles distributed in the ceramic matrix have uneven edges. From the observation of SEM images, it may be concluded that in the case of a composite of the Al_2O_3-Cu-Mo system, the presence of two types of metallic particles (lighter and darker) was noticed. With respect to the Al_2O_3-Cu-Mo composites, further studies have to be done because based on microscopic observations, we are not able to clearly determine which lighter or darker bright areas correspond to which Cu or Mo phases. For this purpose, a chemical analysis of the Al_2O_3-Cu-Mo composite composition was carried out further in the manuscript.

Figure 7 presents the SEM pictures with the microanalysis of the chemical composition made by an energy-dispersive spectroscopy (EDS) technique of Al_2O_3-Cu-Mo. The presence of aluminum, oxygen, nickel, and molybdenum was found. As can be observed, a characteristic is that the copper atoms and molybdenum atoms (blue and pink color respectively) occupy the different areas. It must be remembered that they were added and mixed with alumina as a separate phase so the distribution of phases is relatively homogenous. Direct EDS measurements allowed us to confirm two separate metallic phases in the final material. This result suggested that

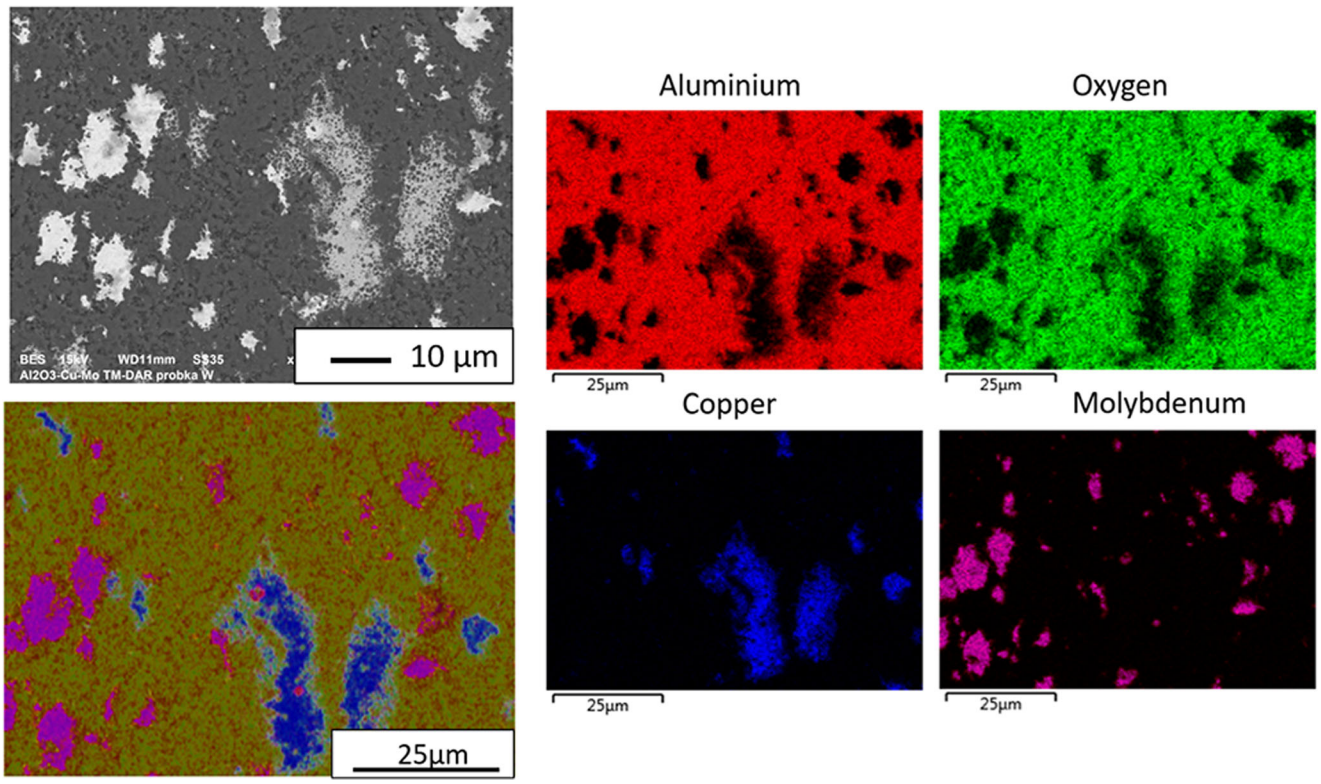

Fig. 7 The microanalysis of the chemical composition of Al_2O_3-Cu-Mo composites

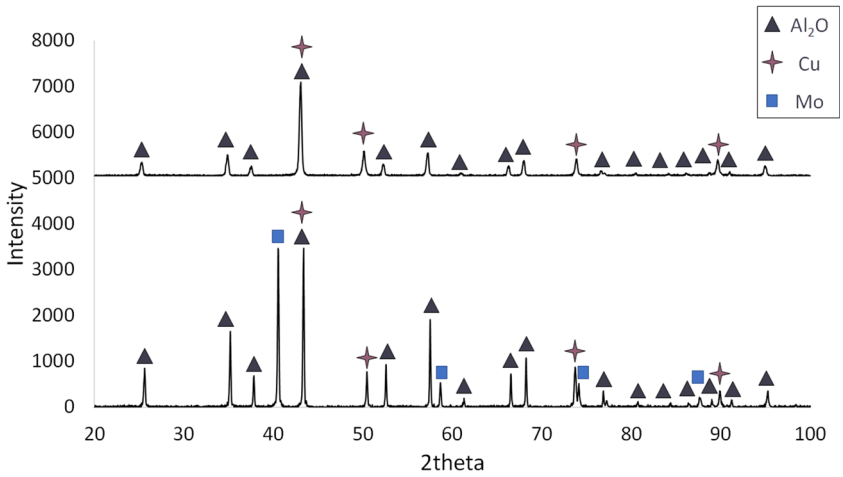

Fig. 8 XRD diffractogram of sintered composites. **a** Al_2O_3-Cu. **b** Al_2O_3-Cu-Mo

during synthesis, the copper and molybdenum particles did not combine and react with each other. To examine the phase composition, X-ray analysis was carried out.

The phase composition of Al_2O_3-Cu and Al_2O_3-Cu-Mo composites sintered in is presented in Fig. 8. The XRD patterns reveal the presence of aluminum oxide and copper in the case of Al_2O_3-Cu materials. In the case of composites from the Al_2O_3-Cu-Mo system, the X-ray analysis provided the information that this system contains three phases such as aluminum oxide, copper, and molybdenum. From the above information of XRD patterns, it may be concluded that the used reducing atmosphere for sintering materials prevents new phases and reactions between components during sintering.

Direct measurements of the obtained XRD results enable us to observe characteristic patterns for composite samples with different chemical compositions. In case of composite specimens from Al_2O_3-Cu system, reflexes at 2θ value equal to 43.06°, 50.09°, 73.86°, 89.66°, and 94.96° correspond to the (111), (200), (220), (311), and (222) Cu atomic planes respectively (#04-001-3178), while reflexes from the same sequence of Cu atomic planes for samples obtained from Al_2O_3-Cu-Mo system were observed at 2θ value equal to 43.37°, 50.44°, 74.14°, 89.89°, and 95.27° in sequence (#04-010-6011). During the analysis, it was also found that in samples obtained with both copper and molybdenum in metal phase, reflexes from 2θ value equal to 40.52°, 58.66°, 73.72°, and 87.63° correspond to the (110), (200), (211), and (220) Mo atomic planes respectively (#04-003-1483). XRD analysis revealed that in both series, metallic components of the composite can be characterized by cubic structure (Fm-3 m for Cu and Im-3 m for Mo) materials preventing new phases and reactions between components during sintering.

It was found that Al_2O_3-Cu composites were described by relative density equal to 96.60 ± 0.74%, while the higher relative density equal to 98.93 ± 0.59% was measured for Al_2O_3-Cu-Mo composites. The higher value of density may be attributed to the addition of molybdenum particles in composites.

The tests of mechanical properties and wear behavior of the obtained composites allowed us to assess the effects of the addition of the molybdenum particles in the Al_2O_3-Cu materials compared to composites without them.

Vickers's hardness and fracture toughness analysis revealed the dependence of the obtained results on the specimens' chemical composition. The Vickers hardness results, shown in Table 1, correlate very well with the obtained relative densities. Samples from the ternary Al_2O_3-Cu-Mo system, prepared with an equal amount of Cu and Mo in the metallic phase, were characterized by higher hardness values in comparison to the reference Al_2O_3-Cu samples. On the basis of results, it was found that average hardness measured for specimens with metallic phase including both Cu and Mo was equal to 10.06 ± 0.49 GPa while for reference samples with Cu, it was equal to 6.81 ± 2.08 GPa. The results obtained (Table 1) provided evidence that molybdenum particles improve the hardness of the composites.

The changes noticed in the sinter fracture toughness are presented in Table 2. Although the Al_2O_3-Cu-Mo composites are distinguished to increase the Vickers's hardness to compare to the Al_2O_3-Cu materials, it does not visibly affect the

Table 1 The results of Vickers hardness measurement of the produced composites

Samples	Al_2O_3-Cu-Mo	Al_2O_3-Cu
Vickers hardness (GPa)	10.06 ± 0.49	6.81 ± 2.08

Table 2 The results of fracture toughness of the produced composites

Samples	Al_2O_3-Cu-Mo	Al_2O_3-Cu
Anstis equation (MPa $m^{0.5}$)	10.63 ± 1.40	10.41 ± 1.24
Niihara equation (MPa $m^{0.5}$)	6.13 ± 0.62	6.04 ± 0.55

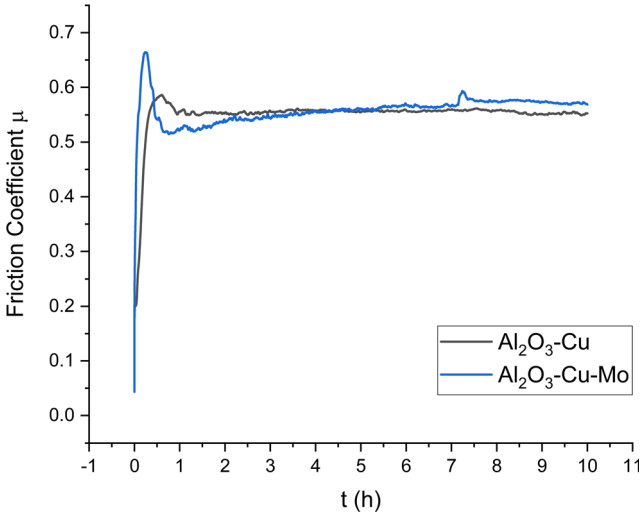

Fig. 9 Sample dependence of the coefficient of friction on time for composite samples Al_2O_3-Cu and Al_2O_3-Cu-Mo composites

fracture toughness of analyzed composites. The results calculated provided information that average K_{1C} values measured, with use of Niihara equation, for composites with and without the addition of Mo in the metallic phase were equal to 6.13 ± 0.62 MPa $m^{0.5}$ and 6.04 ± 0.55 MPa $m^{0.5}$, respectively. The slight enhancement of fracture toughness may be attributed to the Mo particles, acting as stopping either the crack propagation or the crack deflection points appropriately caused by metal ductility.

In addition to the microstructure analysis and its impact on the mechanical properties, the initial tribological test was carried out. The results of pin on ball dry friction test are presented in Fig. 8 for the Al_2O_3-Cu and Al_2O_3-Cu-Mo composites. Direct measurements have shown that the mean value of the coefficient of friction of the tested materials was similar (Fig. 9). The obtained result for Al_2O_3-Cu samples was 0.58 ± 0.05 and the COF of Al_2O_3-Cu-Mo was 0.57 ± 0.08. The value of COF of Al_2O_3Cu stabilized after approximately 1 h while COF of Al_2O_3-Cu-Mo was slightly increasing between the 30th minute and the 7th hour of test, and then reached a plateau.

Results of average wear volume calculations are presented in Fig. 10a. Based on the average wear volume, it can be inferred that the value obtained for Al_2O_3-Cu composite samples was 1.99 ± 0.14 mm^3 while Al_2O_3-Cu-Mo composites equaled to 1.28 ± 0.21 mm^3. It was found that these values were used to determine the specific wear rate. Since this coefficient is related to applied load and sliding distance, it is more universal and makes comparing samples tested in different conditions more reliable. Data collected in our experiment are presented in Fig. 10b. It has been reported that the mean specific wear rates of Al_2O_3-Cu and Al_2O_3-Cu-Mo composite samples were $0.35 \times 10^{-5} \pm 0.02$ mm^3 N^{-1} m^{-1} and $0.22 \times 10^{-5} \pm 0.04$ mm^3 N^{-1} m^{-1} respectively. Molybdenum addition improved wear resistance properties of the material, but even without this compound, tribological test results are very satisfying.

4 Conclusions

The investigations present the fabrication of alumina matrix composites reinforced with copper (series I) and copper and molybdenum (series II). The correlation between the studied microstructures and measured selected properties of the obtained composites was analyzed. Furthermore, the tribological behavior of the fabricated materials was examined.

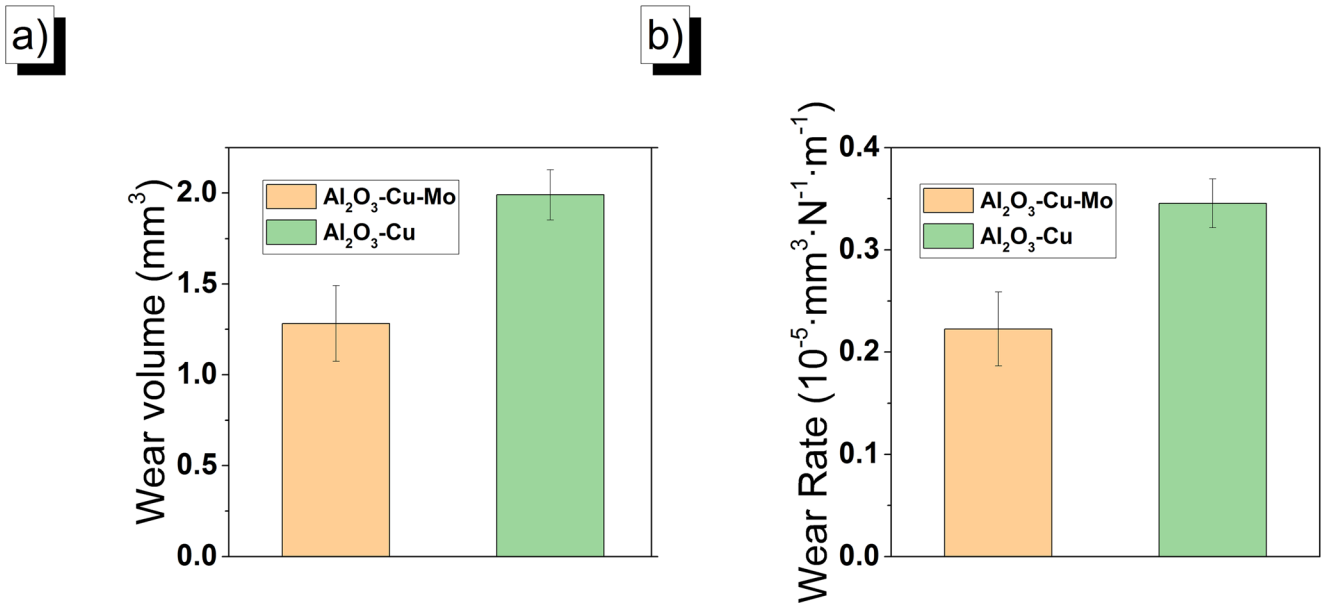

Fig. 10 Comparison of the average. **a** Wear volume. **b** Specific wear rate of composite samples

Obtained results reinforce the potential use of a slip casting method for producing composites from the Al_2O_3-Cu and Al_2O_3-Cu-Mo systems. Based on the sedimentation test, it can be concluded that both suspension examinations in the investigation may be suitable for forming composites by the slip casting method since they are stable for a minimum of 2 h from the moment of mass preparation. The rheological investigations revealed that all of the obtained slurries were non-Newtonian shear diluted fluids. The fabricated composites were subjected to XRD analysis, microstructural observations, and mechanical property measurements. The X-ray investigations provided evidence that in Al_2O_3-Cu and Al_2O_3-Cu-Mo systems, no new phases were revealed after the sintering process. The observations exercised with scanning electron microscopy revealed a good interface of metal particles to alumina matrix in both types of composites. Moreover, based on observation, it was found that the distribution of the metallic phase in obtained specimens has rather a homogeneous character. The experiments demonstrated that the addition of molybdenum in the Al_2O_3-Cu materials caused an increase in hardness without a significant impact on the fracture toughness of obtained composites. The obtained results showed that addition molybdenum to Al_2O_3-Cu system improved wear resistance properties of the material.

The received results gain new notices about the correlation between parameters of the production process and microstructure and properties of the materials of the Al_2O_3-Cu-Mo. The realization of the submitted research methodology provided basic knowledge about producing ceramic-metal composites from the ternary system. Furthermore, the presented results concerning Al_2O_3-Cu-Mo composites are new scientific advance in the fundamental understanding of ternary system of ceramic matrix composite science.

Funding The study was accomplished with the help of the funds allotted by The National Science Centre within the framework of the research project "OPUS 13" no. 2017/25/B/ST8/02036. This investigation is supported by the Foundation for Polish Science (FNP) - START 2019 scholarship.

Compliance with ethical standards

Conflict of interest The authors declare that they have no conflict of interest.

References

1. Travitzky N (2012) Processing of ceramic–metal composites. Adv Appl Ceram 111:286–300. https://doi.org/10.1179/1743676111Y.0000000073
2. Okada A (2003) Ceramic-matrix composites. In: Somiya S, Aldinger F, Claussen N, Spriggs RM, Uchino K, Koumoto K, Kaneno M (eds) Handbook of advance ceramics. Elsevier, Amsterdam, pp 417–443. https://doi.org/10.1016/B978-012654640-8/50042-0
3. Chung DDL (2017) Ceramic-matrix composites. In: Chung DDL (ed) Carbon composites. Elsevier, Amsterdam, pp 467–531. https://doi.org/10.1016/B978-0-12-804459-9.00008-7
4. Zinatloo-Ajabshir S, Salavati-Niasari M (2019) Preparation of magnetically retrievable $CoFe_2O_4$@SiO_2@$Dy_2Ce_2O_7$ nanocomposites as novel photocatalyst for highly efficient degradation of organic contaminants. Compos Part B 174:106930. https://doi.org/10.1016/j.compositesb.2019.106930
5. Zinatloo-Ajabshir S, Zinatloo-Ajabshir Z, Salavati-Niasari M, Bagheri S, Abd Hamid SB (2017) Facile preparation of $Nd_2Zr_2O_7$–ZrO_2 nanocomposites as an effective photocatalyst via a new route. J Energy Chem 26:315–323. https://doi.org/10.1016/j.jechem.2016.11.005
6. Zinatloo-Ajabshir S, Mortazavo-Derazkola S, Salavati-Niasari M (2018) Nd_2O_3–SiO_2 nanocomposites: a simple sonochemical preparation, characterization and photocatalytic activity. Ultrason Sonochem 42:171–182. https://doi.org/10.1016/j.ultsonch.2017.11.026
7. Zinatloo-Ajabshir S, Sadat Morassaei M, Salvati-Niasari M (2019) Facile synthesis of $Nd_2Sn_2O_7$-SnO_2 nanostructures by novel and environment-friendly approach for the photodegradation and removal of organic pollutants in water. J Environ Manag 233:107–119. https://doi.org/10.1016/j.jenvman.2018.12.011
8. Callister WD Jr (2000) Materials science and engineering - an introduction, 5th edn. Anti-Corrosion Methods and Materials 47:1. https://doi.org/10.1108/acmm.2000.12847aae.001
9. Carter CB, Norton MG (2013) Ceramic materials: science and engineering. Springer, New York. https://doi.org/10.1007/978-1-4614-3523-5
10. Zinatloo-Ajabshir S, Baladi M, Amiri O, Salavati-Niasari M (2020) Sonochemical synthesis and characterization of silver tungstate nanostructures as visible-light-driven photocatalyst for wastewater treatment. Sep Purif Technol 248:117062. https://doi.org/10.1016/j.seppur.2020.117062
11. Okada A (2003) Ceramic-matrix composites. In: Somiya S, Aldinger F, Claussen N, Spriggs RM, Uchino K, Koumoto K, Kaneno M (eds) HandbookZinatloo-Ajabshir S, Salehi Z, Salehi Z, Salavati-Niasari M (2018) Green synthesis and characterization of $Dy_2Ce_2O_7$ nanostructures using Ananas comosus with high visible-light photocatalytic activity of organic contaminants. J Alloys Compd 763:314–321. https://doi.org/10.1016/j.jallcom.2018.05.311
12. Mortazavi-Derazkola S, Zinatloo-Ajabshir S, Salavati-Niasari (2017) Facile hydrothermal and novel preparation of nanostructured Ho2O3 for photodegradation of eriochrome black T dye as water pollutant. Adv Powder Technol 28:747–754. https://doi.org/10.1016/j.apt.2016.11.022
13. Razi F, Zinatloo-Ajabshir S, Salavati-Niasari M (2017) Preparation, characterization and photocatalytic properties of Ag_2ZnI_4/AgI nanocomposites via a new simple hydrothermal approach. J Mol Liq 225:645–651. https://doi.org/10.1016/j.molliq.2016.11.028
14. Sun X, Yeomans JA (1996) Microstructure and fracture toughness of nickel particle toughened alumina matrix composites. J Mater Sci 31:875–880. https://doi.org/10.1007/BF00352885

15. Sekino T, Nakajima T, Niihara K (1996) Mechanical and magnetic properties of nickel dispersed alumina-based nanocomposite. Mater Lett 29:165–169. https://doi.org/10.1016/S0167-577X(96)00136-X
16. Sekino T, Nakajima T, Ueda S, Niihara K (2005) Reduction and sintering of a nickel-dispersed-alumina composite and its properties. J Am Ceram Soc 80:1139–1148. https://doi.org/10.1111/j.1151-2916.1997.tb02956.x
17. Nawa M, Sekino T, Niihara K (1994) Fabrication and mechanical behaviour of Al_2O_3/Mo nanocomposites. J Mater Sci 29:3185–3192. https://doi.org/10.1007/BF00356661
18. Díaz LA, Valdés AF, Díaz C, Espino AM, Torrecillas R (2003) Alumina/molybdenum nanocomposites obtained in organic media. J Eur Ceram Soc 23:2829–2834. https://doi.org/10.1016/S0955-2219(03)00295-4
19. Liu DM, Tuan WH (1996) Microstructure and thermal conduction properties of Al_2O_3-Ag composites. Acta Mater 44:813–818. https://doi.org/10.1016/1359-6454(95)00205-7
20. Rodriguez-Suarez T, Díaz LA, Torrecillas R, Lopez-Esteban S, Tuan WH, Nygren M, Moya JS (2009) Alumina/tungsten nanocomposites obtained by Spark Plasma Sintering. Compos Sci Technol 69:2467–2473. https://doi.org/10.1016/j.compscitech.2009.06.022
21. Sekino T, Niihara K (1995) Microstructural characteristics and mechanical properties for Al_2O_3/metal nanocomposities. Nanostruct Mater 6:663–666. https://doi.org/10.1016/0965-9773(95)00145-X
22. Oh ST, Sekino T, Niihara K (1998) Fabrication and mechanical properties of 5 vol% copper dispersed alumina nanocomposite. J Eur Ceram Soc 18:31–37. https://doi.org/10.1016/s0955-2219(97)00099-x
23. Oh ST, Sekino T, Niihara K (1998) Effect of particle size distribution and mixing homogeneity on microstructure and strength of alumina/copper composites. Nanostruct Mater 10:327–332. https://doi.org/10.1016/S0965-9773(98)00072-5
24. Wang L, Shi JL, Lin MT, Chen HR, Yan DS (2001) The thermal shock behavior of alumina-copper composite. Mater Res Bull 36:925–932. https://doi.org/10.1016/S0025-5408(01)00549-9
25. Oh ST, Kang KM (2004) Effect of sintering atmosphere on the microstructure of hot-pressed Al2O3/Cu nanocomposites. Mater Sci Forum 449–452:1217–1220. https://doi.org/10.4028/www.scientific.net/MSF.449-452.1217
26. Oh ST, Lee JS, Sekino T, Niihara K (2001) Fabrication of Cu dispersed Al_2O_3 nanocomposites using Al_2O_3/CuO and Al_2O_3/Cu-nitrate mixtures. Scr Mater 44:2117–2120. https://doi.org/10.1016/S1359-6462(01)00890-9
27. Miranda-Hernández JG, Moreno-Guerrero S, Soto-Guzman AB, Rocha-Rangel E (2006) Production and characterization of Al_2O_3-Cu composite materials. J Ceram Process Res 7:311–314
28. Stratigaki M, Pabst W, Nečina V, Hajíček M, Gotsis AD (2019) Microstructure and mechanical properties study of slip-cast copper–alumina composites. SN Appl Sci 1. https://doi.org/10.1007/s42452-018-0037-4
29. Cahill JA, Kirshenbaum AD (1962) The density of liquid copper from its melting point (1356 K) to 2500 K and an estimate of its critical constants. J Phys Chem 66:1080–1082. https://doi.org/10.1021/j100812a027
30. Darrell Ownby P, Liu J (1988) Surface energy of liquid copper and single-crystal sapphire and the wetting behavior of copper on sapphire. J Adhes Sci Technol 2:255–269. https://doi.org/10.1163/156856188X00264
31. Schmitz J, Brillo J, Egry I (2014) Surface tension of liquid Al-Cu and wetting at the Cu/sapphire solid-liquid interface. Eur Phys J Spec Top 223:469–479. https://doi.org/10.1140/epjst/e2014-02103-5
32. Schmitz J, Brillo J, Egry I (2010) Surface tension of liquid Cu and anisotropy of its wetting of sapphire. J Mater Sci 45:2144–2149. https://doi.org/10.1007/s10853-010-4212-2
33. Hsissou R, Berradi M, El Bouchti M, El Bachiri A, El Harfi A (2019) Synthesis characterization rheological and morphological study of a new epoxy resin pentaglycidyl ether pentaphenoxy of phosphorus and their composite (PGEPPP/MDA/PN). Polym Bull 76:4859–4878. https://doi.org/10.1007/s00289-018-2639-9
34. Szafran M, Konopka K, Bobryk E, Kurzydłowski KJ (2007) Ceramic matrix composites with gradient concentration of metal particles. J Eur Ceram Soc 27:651–654. https://doi.org/10.1016/j.jeurceramsoc.2006.04.046
35. Konopka K, Ozi bło A (2001) Microstructure and the fracture toughness of the Al_2O_3-Fe composites. Mater Charact 46:125–129. https://doi.org/10.1016/S1044-5803(01)00113-9
36. Gong Y, Tian W, Zhang P, Chen J, Zhang Y, Sun Z (2019) Slip casting and pressureless sintering of Ti_3AlC_2. J Adv Ceram 8:367–376. https://doi.org/10.1007/s40145-019-0318-4
37. Hsissou R, Elharfi A (2020) Rheological behavior of three polymers and their hybrid composites (TGEEBA/MDA/PN), (HGEMDA/MDA/PN) and (NGHPBAE/MDA/PN). J King Saud Univ Sci 32:235–244. https://doi.org/10.1016/j.jksus.2018.04.030
38. Hsissou R, Dagdag O, Berradi M, El Bouchti M, Assouag M, Elharfi A (2019) Development rheological and anti-corrosion property of epoxy polymer and its composite. Heliyon 5:e02789. https://doi.org/10.1016/j.heliyon.2019.e02789
39. Hsissou R, El Bouchti M, El Harfi A (2017) Elaboration and viscosimetric, viscoelastic and rheological studies of a new hexafunctional polyepoxide polymer: hexaglycidyl ethylene of methylene dianiline. J Mater Environ Sci 8:4349–4361. https://doi.org/10.26872/jmes.2017.8.12.458
40. Hsissou R, Bekhta A, El Harfi A (2017) Viscosimetric and rheological studies of a new trifunctional epoxy pre-polymer with noyan ethylene: triglycidyl ether of ethylene of bisphenol A (TGEEBA). J Mater Environ Sci 8:603–610
41. Bekhta A, Hsissou R, Berradi M, El Bouchti M, Elharfi A (2019) Viscosimetric and rheological properties of epoxy resin TGEUBA and their composite (TGEUBA/MDA/TGEMDA+TSP). Result Eng 4:100058. https://doi.org/10.1016/j.rineng.2019.100058
42. Hsissou R, Bekhta A, El Bachiri A, Rafik M, Elharfi A (2020) Rheological properties of composite polymers and hybrid nanocomposites. Heliyon. 6:e04187. https://doi.org/10.1016/j.heliyon.2020.e04187
43. Niihara K (1983) A fracture mechanics analysis of indentation-induced Palmqvist crack in ceramics. J Mater Sci Lett 2:221–223. https://doi.org/10.1007/BF00725625
44. Niihara K, Morena R, Hasselmann DPH (1982) Evaluation of K_{IC} of brittle solids by indentation method with low crack-to-indent ratios. J Mater Sci 1:13–16
45. Anstis GR, Chantikul P, Lawn BR, Marshall DB (1981) A critical evaluation of indentation techniques for measuring fracture toughness: I, direct crack measurements. J Am Ceram Soc 64:533–538. https://doi.org/10.1111/j.1151-2916.1981.tb10320.x
46. Nastic A, Merati A, Bielawski M, Bolduc M, Fakolujo O, Nganbe M (2015) Instrumented and Vickers indentation for the characterization of stiffness, hardness and toughness of zirconia toughened Al_2O_3 and SiC armor. J Mater Sci Technol 31:773–783. https://doi.org/10.1016/j.jmst.2015.06.005